Partial Grain Refinement in Al-3%Cu Alloy during ECAP at Elevated Temperatures

Inna Mazurina[1], Taku Sakai[1], Hiromi Miura[1], Oleg Sitdikov[1,2] and Rustam Kaibyshev[3]

[1]*Department of Mechanical Engineering and Intelligent Systems, UEC Tokyo (The University of Electro-Communications), Tokyo 182-8585, Japan*
[2]*Institute for Metals Superplasticity Problems, Khalturina 39, Ufa 450001, Russia*
[3]*Belgorod State University, Belgorod 308034, Russia*

Microstructural changes during equal channel angular pressing (ECAP) in a temperature interval from 523 to 748 K (~0.6–0.8 T_m) were studied in a coarse-grained binary aluminum alloy Al-3%Cu. Hot ECAP results in grain refinement taking place at all temperatures investigated, leading to a non-uniform development of deformation-induced fine grains and the remnant original grains containing subgrains with low-angle boundaries. Fine-grained structure is developed along microshear bands formed in grain interiors as well as along initial grain boundaries. The number and the average misorientation angle of the boundaries of microshear bands start to increase at above a critical strain of about 2, finally leading to development of new fine-grained structures. The volume fraction and the average misorientation of deformation-induced boundaries are reduced with rising temperature. The thermal stability of the evolved deformation microstructures and several factors controlling grain refinement during hot ECAP are discussed in details.

Keywords: *grain refinement, temperature effect, microshear band, equal channel angular pressing (ECAP), aluminum alloy*

1. Introduction

In recent years, there has been an increasing interest in the production of ultrafine-grained (UFG) materials by means of severe plastic deformation (SPD) for both commercial and investigative purposes.[1)] Several SPD techniques such as equal channel angular pressing (ECAP),[1–20)] torsion under high pressure[1,3,21)] and multi-directional forging (MDF)[22–28)] are now available for attaining of the UFG structures in numerous metals and alloys. There are several reports to date dealt with the investigation of the fine-grained structure evolution in Al alloys at different temperatures during SPD.[2–4,6,8,9,11–14,16,18–22,24–26)] Under severe plastic deformation conditions, fragmentation of original grains takes place at medium strains followed by *in-situ* formation of fine crystallites at high strains, which is sometimes called as continuous dynamic recrystallization (CDRX).[9,16,18–20,22,24,25)] Such structural changes in Al alloys during SPD are mostly investigated at ambient temperature and only few studies address high-temperature SPD and UFG formation at elevated temperatures.[6,8–10,12,13,16,18–20,24–26)]

The present authors have investigated the microstructural evolution in Al alloys during hot SPD in the recent works.[9,12,16,18–20,24,25)] Multi-component commercial-based Al alloys were used for these investigations, because both thermally stable dispersion particles and soluble precipitations coexist in a wide temperature range. It has been shown that the deformation microstructures having high density of dislocations can be easily developed and kept in such alloys due to a pinning effect of the particles. The latter may strongly inhibit the rate of dynamic recovery and provide a high thermal stability of deformation microstructures.[9,12,16,24,25)] As a result, rather fine-grained structures with the moderate dislocation density can be formed at large strains even at high temperatures. On the other hand, such microstructural changes may be different from those in more pure Al alloys without any dispersion particles, because the microstructures evolved may be characterized by a low thermal stability at high temperatures.[8)] The main features of the microstructural evolution in such alloys during hot SPD, however, have been not still studied in sufficient details.

The aim of the present work was to study the microstructural changes taking place during hot ECAP of a coarse-grained binary alloy Al-3%Cu. The microstructural evolution and mechanisms of new grain formation were investigated mainly at a temperature of 523 K. The misorientation characteristics of deformation-induced boundaries and the other parameters of the evolved microstructures were studied in details at various strains up to 12. An influence of increasing the deformation temperature in the interval from 523 to 748 K (~0.6–0.8 T_m) on grain refinement process is also analyzed and discussed.

2. Experimental Procedure

A binary aluminum alloy Al-3%Cu (in mass%) used in the present work was produced by direct chill casting. The alloy was homogenized at 793 K for 4 h as a solution treatment, followed by cooling with a rate of about 50 K/h leading to formation of relatively coarse particles of Al_2Cu (θ-phase) and Al-0.1%Cu matrix at room temperature.[29)] Note that such preliminary heat treatment regime was especially selected for this alloy to avoid any effects of deformation temperature on precipitation and analyze only the microstructural evolution during ECAP. The initial microstructure was composed of roughly equiaxed coarse grains with the grain size varied from 100 to 350 μm (Fig. 1(a)). The precipitates of θ-phase showed round platelet shape and the size ranging from 0.5 to 1 μm (Fig. 1(b)). Samples for ECAP were machined into rods with a diameter of 20 mm and a length of 100 mm. ECAP was conducted at temperatures from 523 to 748 K using an isothermal die with a circular internal cross-section with a diameter of 20 mm. The channel had an L-shaped configuration with an angle of intersection of 90° and that at

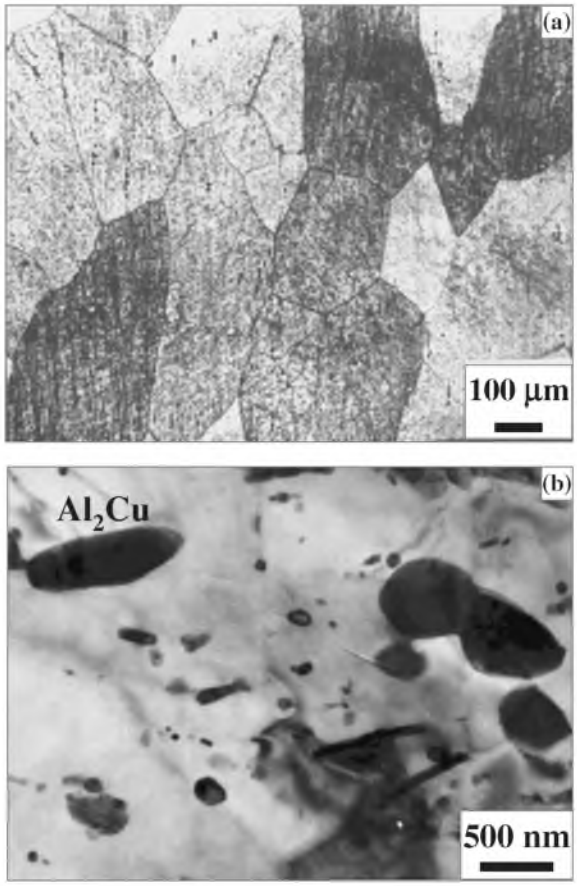

Fig. 1 Initial microstructure of Al-3%Cu alloy before ECAP. (a) Optical and (b) TEM micrographs.

the outer arc curvature of 0°. Deformation through this channel produced a strain of about $\varepsilon = 1$ upon each pass through the die.[2] The samples were pressed repeatedly to strains of about 12 using route A, *i.e.* without rotation of the billet in each pass. This route, being the most effective one for formation of fine-grained structure with high angle boundaries (HABs),[12] has been used in the author's previous works[9,12,16,18–20] and applied here to provide some compatible data.

The pressed samples were quenched in water after each ECAP pass and finally cut parallel to the pressing direction in longitudinal section for microstructural observation. Metallographic analysis was carried out using an optical microscope (OM) after etching by the standard Dics-Keller reagent. The orientation imaging microscopy (OIM) with automated indexing of electron back scattering diffraction (EBSD) patterns was performed in LEO-1530 scanning electron microscope (SEM) with OIM analysis software provided by HKL Technology, Inc. The misorientation distributions of deformation-induced boundaries were derived from EBSD technique. The boundaries with misorientation less than 2° were not taken into account. On the other hand, thin discs with a diameter of 3 mm for transmission electron microscopy (TEM) examination were mechanically thinned and then electropolished in a solution of 30% HNO_3 and 70% CH_3OH at about −30°C using a Tenupol-3 twin-jet polishing unit. Foils were examined using a JEOL-2000EX TEM.

3. Results

3.1 Microstructural evolution at 523 K

3.1.1 Deformation microstructure

Typical OM microstructures developed in Al-3%Cu alloy during ECAP at 523 K are shown in Fig. 2. It is remarkable to see that the deformed microstructures are highly inhomogeneous even at a final strain of 12. Microstructures developed after the first passage are mainly characterized by elongated initial grains aligned roughly parallel to the pressing direction (PD), in interiors of which deformation bands (DBs) are formed frequently and heterogeneously (Fig. 2(a) and 2(b)). These bands evolved in aluminum alloy are found to be mainly microshear bands (MSBs), the characteristics of which are described elsewhere.[19,20,25,30] The longitudinal grain size and the apparent width of these MSBs are over 400 μm and varied from 6 to 40 μm, respectively. Deformation in the strain interval from 4 to 8 leads to an increase in number of MSBs (Fig. 2(c) and 2(d)), finally leading to a roughly full development of a fine granular structure in the regions with high density of MSBs. It is clearly seen in Figs. 2(d) and 2(e) that such deformed microstructures are inhomogeneously distributed in original grain interiors even at high strains.

Typical orientation imaging microscopy (OIM) maps and the corresponding misorientation profiles are represented in Figs. 3 and 4, respectively. Figure 4 shows typical distributions of point-to-point ($\Delta\Theta$) and cumulative (point-to-origin, $\Sigma\Delta\Theta$) misorientations developed along test lines indicated in Fig. 3. The values of $\Delta\Theta$ and $\Sigma\Delta\Theta$ define the misorientations evolved by 1 μm step relative to the previous point and to the first point, respectively. It can be seen from Fig. 3(a) that new fine grains are inhomogeneously formed in grain interiors. These grains with boundaries of moderate-to-high misorientation angles are evolved in colony in coarse grain interiors in the left hand side of Fig. 3(a) (see along the line A_1), while, as denoted by the line A_2, long-distance straight LABs with low misorientation angles are developed in the right hand side. The misorientation changes along the line A_2 show that low-to-moderate angle boundaries are inhomogeneously developed across grain interiors over a distance of about 30 μm (Fig. 4(b)). These low angle boundaries ranging from 5 to 10° may correspond to those for dislocation subboundaries and embryos of MSBs,[19,20] which will be discussed later.

With further deformation to high strains, the boundaries of such embryos of MSBs may transform to macroscopic and long-distance MSBs, the boundaries of which have high angle misorientations of more than 15°. The number and misorientation of these boundaries increase with deformation and the boundaries are pinched off in the length of fine grains, leading to new fine crystallites developed along these boundaries (Fig. 3(b)). As a result, the microstructures developed at $\varepsilon = 8$ consist of the regions of new fine grains with HABs and parts of original grains containing subgrains with LABs as well as the boundaries of MSBs with moderate angles (Fig. 4(c)). Further deformation to $\varepsilon = 12$ leads to an increase in the volume fraction of fine grains with HABs developed in places with high density of MSBs, while some parts of original grains containing mainly subgrains with

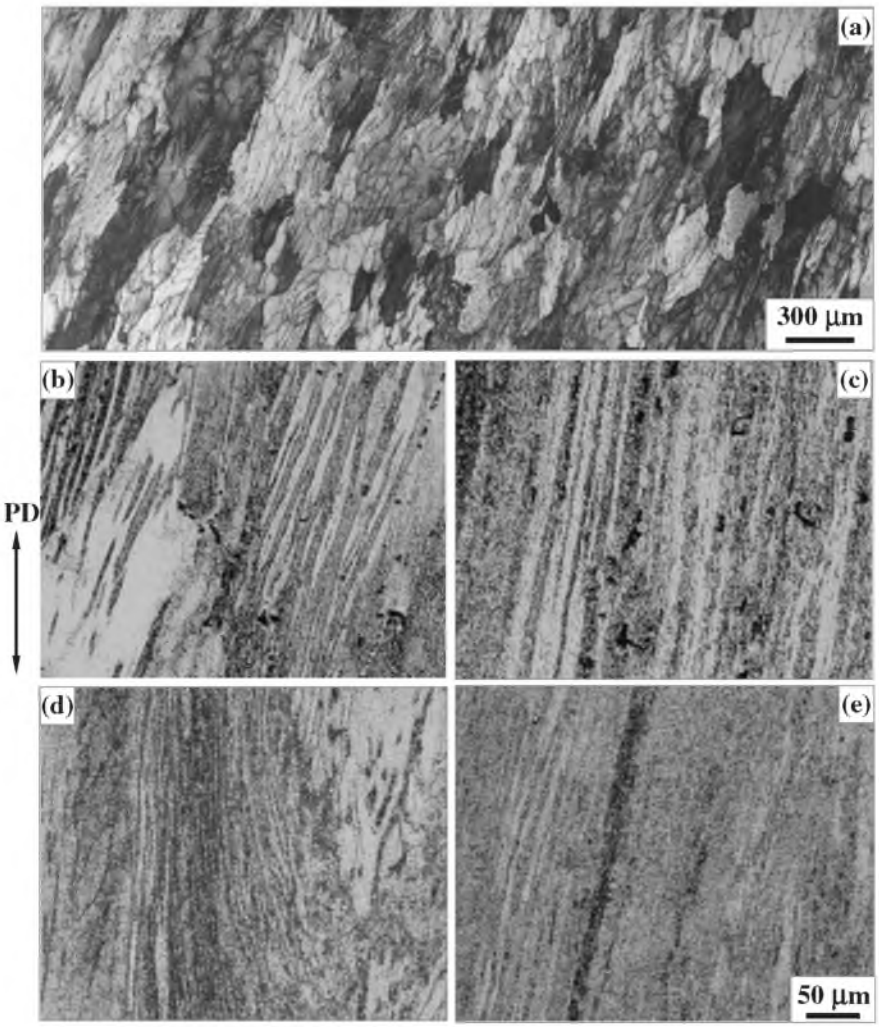

Fig. 2 Optical micrographs of Al-3%Cu alloy deformed by ECAP at 523 K up to strains: (a) $\varepsilon = 1$ (b) $\varepsilon = 2$, (c) $\varepsilon = 4$, (d) $\varepsilon = 8$, (e) $\varepsilon = 12$.

LABs still exist in the right hand side in Fig. 3(c) (see also Fig. 4(d)). It is concluded that, even at $\varepsilon = 12$, fine grains with HABs are not fully evolved in Al-3%Cu alloy ECAPed at 523 K.

Strain dependence of the average grain sizes in the regions of newly developed grains is represented in Fig. 5. The minimum width or spacing of MSBs is also plotted against strain in this figure. The average sizes of crystallites were measured in both the transverse and longitudinal directions of developed microstructures, *i.e.* in the direction of elongated grains (see Fig. 3). It is seen that the longitudinal grain size and the width of MSBs tend to decrease rapidly at low strains below $\varepsilon = 4$ and then gradually with increasing strain, while the transverse grain size does not change significantly. It is interesting to note here that the transverse size of newly developed grains is about two times less than the width of MSBs formed in strain interval from 4 to 8. These three parameters approach to a similar value of about 5 μm at $\varepsilon = 12$ within experimental scatters. Such a good coincidence of the crystallite size and MSBs spacing suggests that dynamic formation of these new grains may be closely connected with the development of MSBs.

3.1.2 Misorientation characteristics of microstructure

Changes in the misorientation distribution of deformation-induced boundaries are represented in Fig. 6. The distributions developed at $\varepsilon = 1$ and 2 are characterized by a high fraction of LABs, so that the histograms plotted have a single peak at around 4°. Some HABs start to develop at $\varepsilon = 3$ due to the evolution of boundaries of MSBs and formation of new fine grains, as confirmed in Fig. 3(a). As a result, the distributions of deformation-induced boundaries are shifted to the regions of HABs and show two peaks corresponded to LABs and HABs at moderate and high strains. Note that such bimodal distribution with some fraction of LABs that exist even at high strains is a very common feature of deformation-induced microstructure misorientation.[31]

Strain dependence of the average misorientation angle (Θ_{av}), the fraction of HABs with misorientation angle above 15° (F_{HAB}) and the volume fraction of new grains (V_{UFG}) are shown in Fig. 7. The average misorientation does not exceed 5° and remains constant at early deformation from $\varepsilon = 1$ to 2, and then starts to increase rapidly at moderate strains of 3 and 4. With further straining, the Θ_{av} continues to increase gradually to ~25° at $\varepsilon = 12$ (Fig. 7(a)). On the other hand, both the fraction of HABs and the volume fraction of new grains start to rise at $\varepsilon \geq 2$ and approach a saturation value of about 0.5 at $8 \leq \varepsilon \leq 12$ (Fig. 7(b)). This suggests that the

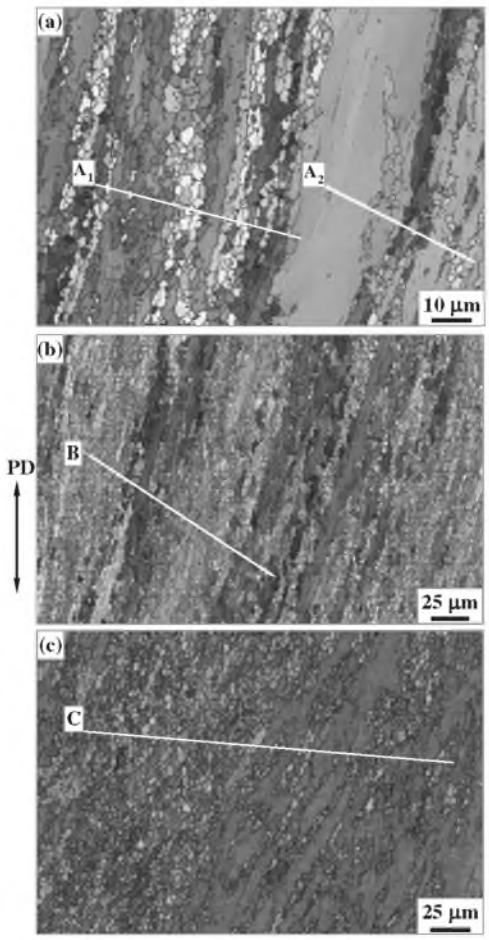

Fig. 3 Typical OIM micropgraphs of Al-3%Cu alloy deformed at 523 K to various strains: (a) $\varepsilon = 3$, (b) $\varepsilon = 8$, (c) $\varepsilon = 12$. Gray and black lines correspond to the boundaries with misorientation from 5° to 15° and >15°, respectively.

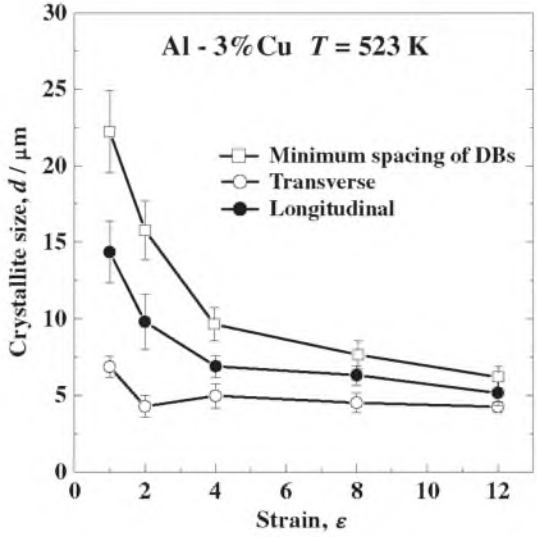

Fig. 5 Changes in crystallite size with strain for Al-3%Cu. Transverse and longitudinal sizes were measured in perpendicular and parallel directions of developed microstructure.

parameters Θ_{av}, F_{HAB} and V_{UFG} have some close connection between each other and strain-induced grain formation starts to take place at strains beyond a critical strain of about 2. In other words, the gradual increase in the Θ_{av}, F_{HAB} and V_{UFG} at large strain can be resulted from high density of MSBs developed in original grain interiors during SPD.

3.1.3 TEM microstructures

Typical microstructures developed at various strains are represented in Fig. 8. It can be seen in Fig. 8(a) that ECAP to $\varepsilon = 2$ leads to development of parallel bands of subgrains having low misorientation angles less than 5°, as suggested

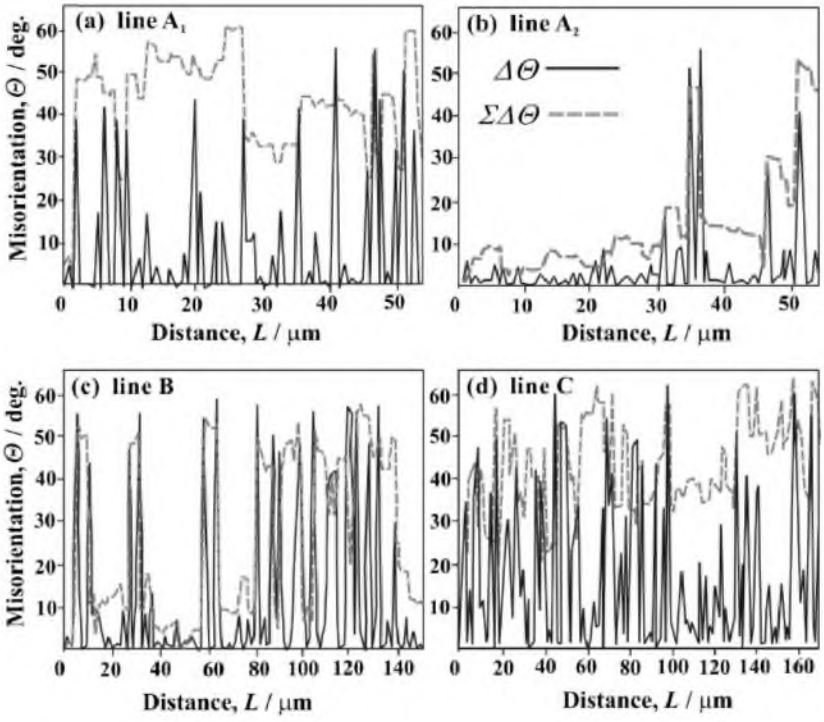

Fig. 4 Point-to-point ($\Delta\Theta$) and cumulative ($\Sigma\Delta\Theta$) misorientations of strain-induced boundaries developed along lines marked in Fig. 3: (a) and (b) $\varepsilon = 3$, (c) $\varepsilon = 8$, (d) $\varepsilon = 12$.

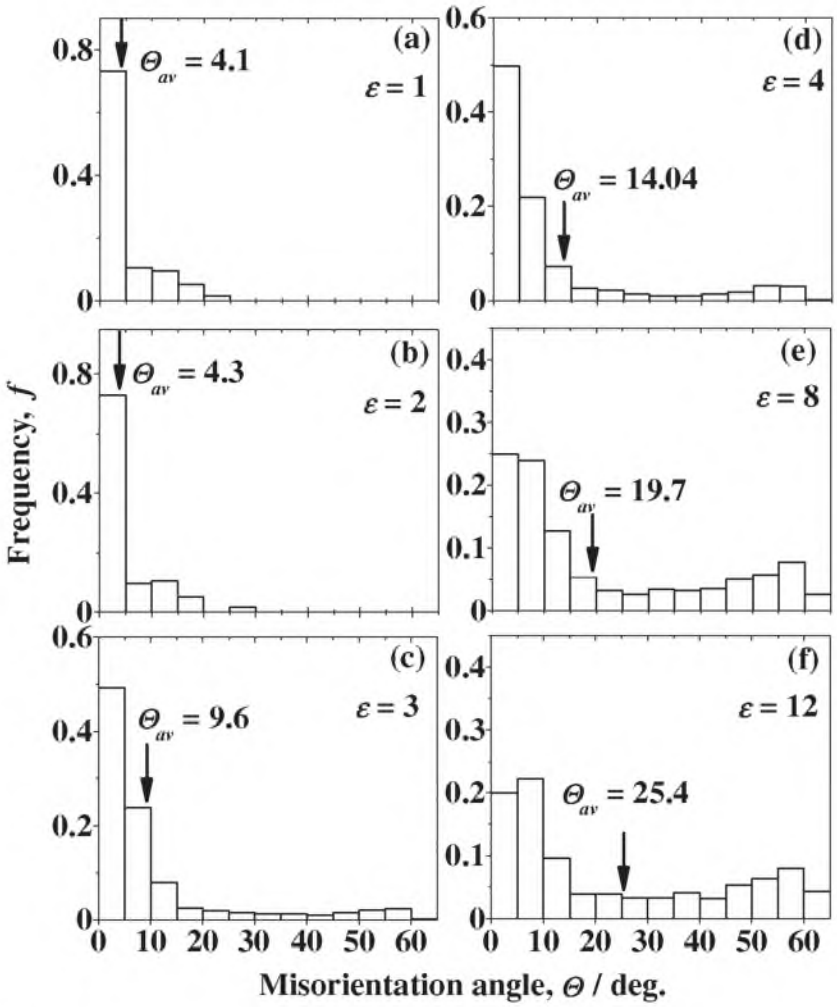

Fig. 6 Changes in the misorientation distribution of deformation-induced boundaries developed in Al-3%Cu alloy deformed by ECAP at 523 K.

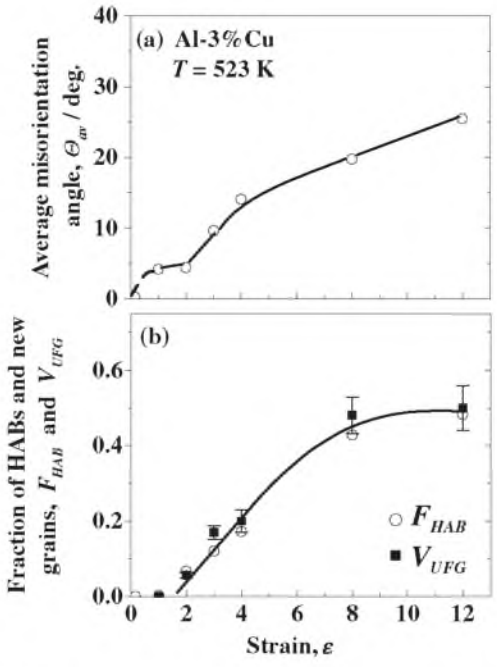

Fig. 7 Changes in (a) the average misorientation angle Θ_{av} and (b) the fraction of strain-induced HABs, F_{HAB} as well as the volume fraction new grains V_{UFG} with repeated ECAP at 523 K for Al-3%Cu alloy.

by single spot electron diffraction (SAED) pattern obtained in 6 μm diameter. Further straining to $\varepsilon = 8$ provides a formation of roughly equiaxed (sub)grained structure, which can be resulted from gradual breaking-up of the bands described above (Fig. 8(b)). The SAED pattern suggests that most of these boundaries have high misorientation angles. After 12 passes of ECAP, roughly equiaxial (sub)grains surrounded by HABs are formed (Fig. 8(c)). There are rather coarse precipitates of θ-phase distributed roughly homogeneously in elongated bands and (sub)grain interiors and also along the boundaries developed in Fig. 8. It is interesting to note here that the particle size in Fig. 8(a) is remarkably smaller than that of coarse precipitates present in the original structure (Fig. 1(b)). This may suggest that the initial coarse Al_2Cu precipitates are *fragmented* and/or *dissolved and re-precipitated* on developed dislocation substructures at earlier stages of ECAP.[15,17]

3.2 Temperature effect on microstructural development

3.2.1 Microstructures developed at high strain

Typical OIM maps developed at a strain of 12 at various temperatures from 573 to 748 K are represented in Fig. 9. The microstructure formed at 573 K looks like roughly equiaxed fine (sub)grains with HABs in a whole volume.

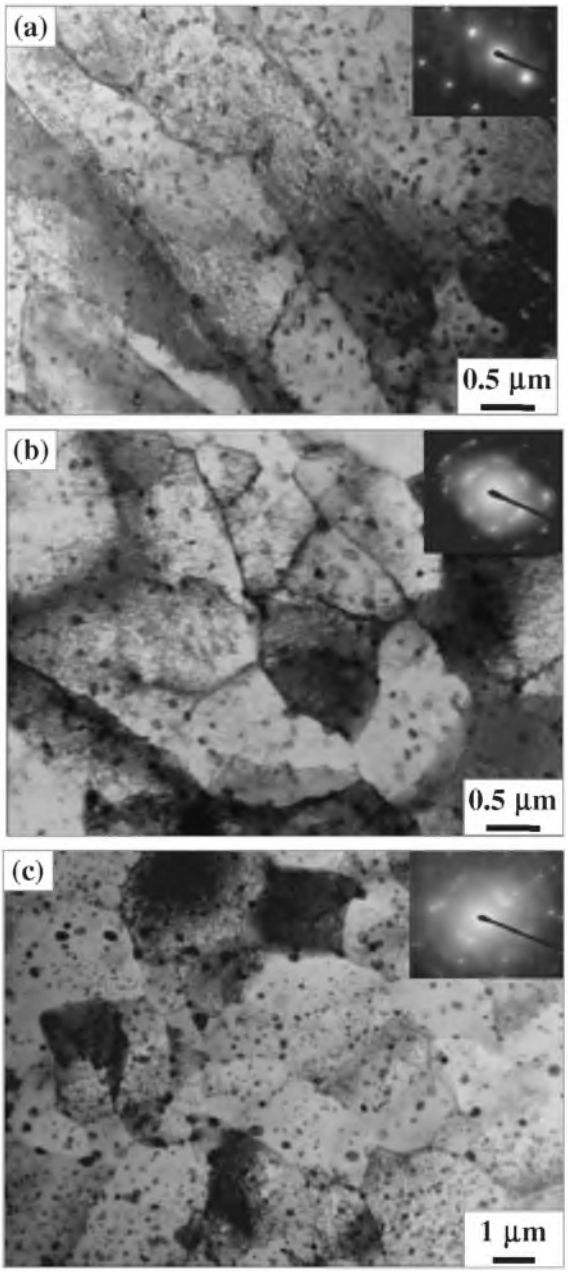

Fig. 8 Transmission electron micrographs of Al-3%Cu alloy deformed by ECAP at 523 K up to strains: (a) $\varepsilon = 2$ (b) $\varepsilon = 8$, (c) $\varepsilon = 12$.

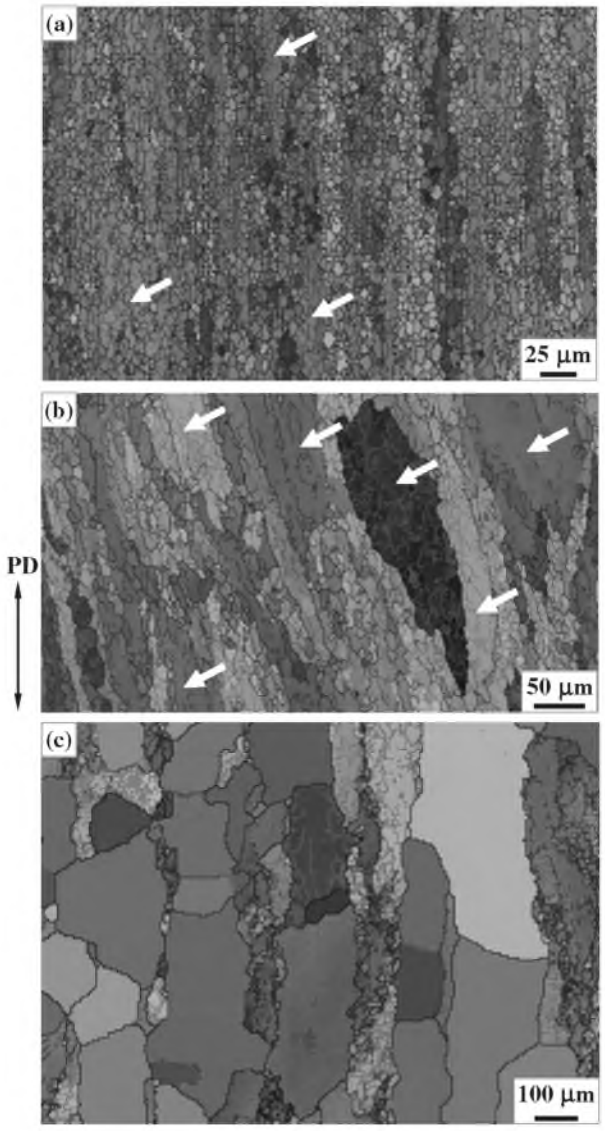

Fig. 9 Typical optical micrographs of Al-3%Cu alloy deformed up to strain 12 at various temperatures: (a) 573 K, (b) 673 K, (c) 748 K. Gray and black lines correspond to the boundaries with misorientation from 5 to 15° and >15°, respectively.

Subgrains with a rather coarse size and LABs are, however, developed in some elongated grain interiors between them, as indicated by arrows in Fig. 9. The volume fraction of such subgrain structures increases with increasing temperature. Further increasing temperature to 748 K results in the formation of very coarse grains having almost no dislocation substructures and a few regions with fine grains surrounded by HABs (Fig. 9(c)). The former may be developed not only by dynamic recovery, but also by interpass static annealing taking place during ECAP.[18] The average interpass time under the present ECAP conditions was 45 min at each temperature. On the other hand, the temperature at solubility limit (solvus) line for Al-3%Cu alloy is around 730 ± 3 K, as it can be obtained from the equilibrium diagram.[29] This heat treatment can result in dissolution of Al_2Cu particles and so, decrease the thermal stability of deformation-induced substructures, leading to static recrystallization during ECAP at 748 K.

3.2.2 Quantitative analysis of deformed microstructures

The misorientation distributions for deformation-induced boundaries, measured only in the fine-grained regions developed at a strain of 12, are represented in Fig. 10. It can be seen that the shape of the distributions is bimodal at each temperature and does not change with increasing temperature even at 748 K. The percentage of HABs with misorientations over 15° as well as the average misorientation angle is gradually decreased with increasing temperature.

Figure 11 shows the temperature dependencies of (a) the grain size, d_{fine}, and (b) the average misorientation angle, Θ_{av}, measured in the regions of fine grains. The data for a commercial 2219 Al alloy obtained at the same ECAP conditions[20] are plotted in Fig. 11 for reference. It can be seen that the size of deformation-induced grains in Al-3%Cu alloy tends to grow with increasing deformation temperature and, in contrast, their boundary misorientation gradually

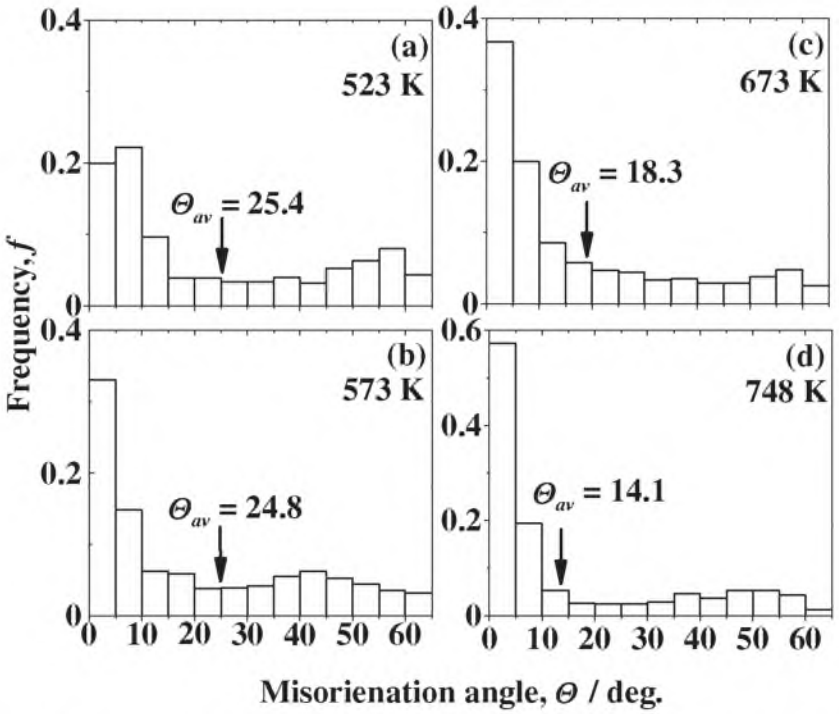

Fig. 10 Misorientation distributions for deformation-induced boundaries developed at $\varepsilon = 12$ in Al-3%Cu alloy after ECAP at various temperatures.

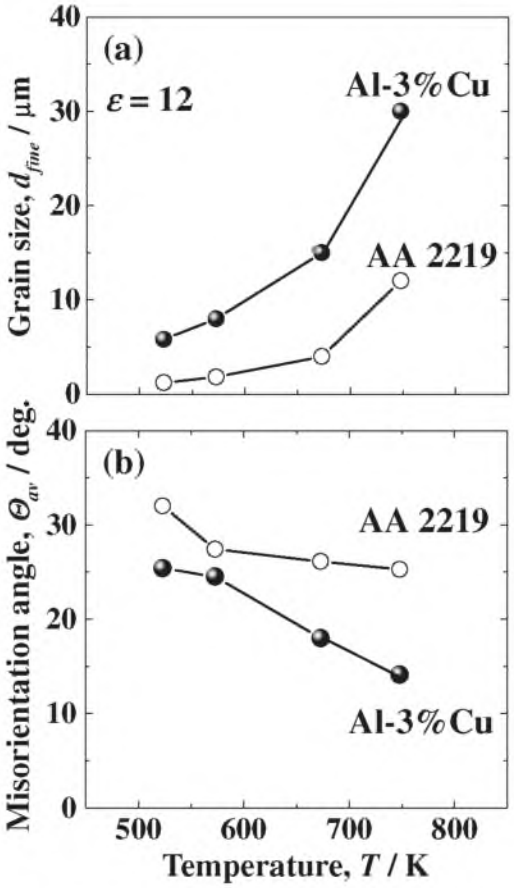

Fig. 11 Changes in (a) average grain size, d_{fine}, and (b) average misorientation angle, Θ_{av}, in the regions of deformation-induced grain structure developed in Al-3%Cu alloy at various temperatures after ECAP at $\varepsilon = 12$. The data for AA 2219 deformed at the same conditions are shown for reference.[20]

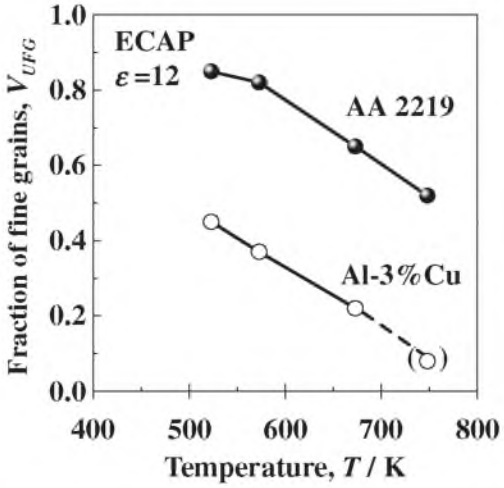

Fig. 12 Temperature dependence of the volume fraction of new fine grains V_{UFG} developed at $\varepsilon = 12$ in Al-3%Cu alloy. The data for AA 2219 deformed at the same conditions are shown for reference 20).

decreases. It is interesting to note that the smaller d_{fine} evolved in the 2219 Al alloy increases at a remarkably slower rate and the Θ_{av} of deformation-induced boundaries does not change even at high temperatures, comparing with those for the Al-3%Cu alloy.

The temperature dependencies of the volume fraction of new fine grains, V_{UFG}, developed at $\varepsilon = 12$ in these alloys are represented in Fig. 12. The V_{UFG} for Al-3%Cu alloy at 748 K is shown with a parenthesis because it may be affected by recrystallization (see Fig. 9(c)). The fractions of fine grains developed in the Al-3%Cu and 2219 Al alloys approach maximum values 0.5 and 0.85 at 523 K, respectively, and decrease rapidly with increasing deformation temperature.

It is concluded, therefore, that strain-induced fine grains are not developed completely during warm-to-hot ECAP and there may be a limit of strain-induced grain formation in both the alloys at high temperatures. Note also that the V_{UFG} for the 2219 Al alloy remains significantly larger at all temperatures investigated. Such influence of temperature on the microstructural parameters developed during ECAP will be discussed in details in the next sections.

4. Discussion

4.1 Strain-induced grain refinement process

The experimental results described above show that grain refinement takes place in the Al-3%Cu alloy during ECAP at 523–748 K. It can be suggested in the results of Figs. 2, 3, 5 and 7 that the mechanism of fine grain formation may be directly associated with MSBs evolved during ECAP. Note that these results may be similar to the characteristics of substructural development and grain refinement taking place, for instance, during cold rolling of Al-0.1%Mg alloy,[30] room-temperature ECAP of Al-0.13%Mg alloy[14] and during multi-directional forging at low, intermediate and high temperatures in pure copper,[27] Fe-20%Cr alloy[28] and 7475 Al alloy,[24,25] respectively. It has been pointed out in these works that grain refinement process taking place during SPD may be related to evolution of MSBs, which are inhomogeneously formed by dynamic relaxation of strain gradients developed in grain interiors, irrespectively of deformation mode and temperature.[9,24,25,28]

The present authors investigated the process of new grain formation due to development of MSBs in a commercial Al alloy 2219 during ECAP at 523–748 K.[19,20] The main results are briefly summarized here. The microstructural changes during ECAP can be subdivided in three stages: *i.e.* an incubation period for new grain evolution in stage 1; grain fragmentation by frequent development of MSBs in stage 2 and continuous development of new grains in stage 3. In stage 1, below a critical strain, $\varepsilon_c \approx 2$, conventional dislocation substructures with LABs are homogeneously developed accompanied by numerous boundaries with low-to-moderate misorientation angles appearing as embryos of MSBs. These contain elongated substructures with misorientation angles of $5^\circ \leq \Theta \leq 15^\circ$, while conventional equiaxed subgrains with LABs of $\Theta \leq 5^\circ$ are developed in the exteriors of MSBs. In stage 2, such embryos can transform into macroscopic MSBs. The number and the average misorientation of the boundaries of MSBs rapidly grow with increasing the deformation, leading to fragmentation of original grain into different misoriented regions. In stage 3, new grains surrounded by HABs are fully developed in a whole volume.

The similar sequence of the structural changes can be observed in the current Al-3%Cu alloy (see Figs. 2–7). Namely, the boundaries of MSBs with low-to-moderate misorientations, introduced by early deformation, start to transform into HABs at above a critical strain of $\varepsilon_c \approx 2$ with repeated ECAP. The value of $\varepsilon_c \approx 2$ does not depend on not only temperature, but also the chemical composition of Al alloys.[19,20] The crystal orientation of each band is frequently alternated and changed discontinuously at the boundaries of MSBs, as seen in Figs. 4(a) and 4(b). This is reasonably consistent with a rigid local lattice rotation akin to kinking.[30,31] Such bands may be roughly categorized as those with transition boundaries having persistent nature. Hence, they are introduced by mechanical working and thus, are mainly controlled by athermal processes.[20,27,28] It has been pointed out[20] that the development of fine-grains regions accompanied by such MSBs can be scarcely influenced by pressing temperature in stages 1 and 2.

On the other hand, the boundaries of MSBs introduced at stages 1 and 2 are rather non-equilibrium and diffuse interfaces[1,14] (see Fig. 8). Dynamic recovery that occurs with higher rate at elevated temperatures can assist the transformation of such strain-induced non-equilibrium boundaries to more equilibrium ones, leading to a more rapid formation of new grains. Repeated deformation to large strains can give enough time for dislocation rearrangement in strain-induced boundaries, leading to both an increase of grain boundary misorientation and a decrease of dislocation density in (sub)grain interiors.[20,27,28,31] Thus, the strain-induced grain formation may be controlled by a dynamic formation of non-equilibrium moderate-to-high angle boundaries in stages 1 and 2, and subsequently by frequent operation of dynamic recovery in these boundaries at large strains (*i.e.* in stage 3). Microstructure changes in stage 3 are, therefore, considered to be controlled by thermally activated rate processes.[27,28,31] It is important to note in Figs. 5–7 that the values of V_{UFG}, F_{HABs} and Θ_{av} are gradually increased during grain refinement, while the average crystallite size developed in fine grained regions retains essentially stable at moderate and high strains. Such dependencies may be considered to be specific features of strain–induced grain structures, typical of cDRX.[22,31] It can be concluded, therefore, that new fine grains evolved during warm-to-hot ECAP of the present Al alloy are resulted from a series of strain-induced continuous reactions; this is essentially similar to cDRX.

4.2 Controlling factors of strain-induced grain refinement

It can be seen in Figs. 9–12 that (i) there is a limit of grain refinement in a dilute Al alloy at elevated temperatures, *i.e.* grain refinement occurs incompletely even after SPD to large strains, leading to non-uniform development of deformation-induced fine grains with HABs and the remnant original grains containing subgrains with LABs; (ii) the volume fraction and the average misorientation angle of deformation-induced grains are reduced with increasing temperature. These results are roughly similar to those for commercial 2219 Al alloy at the similar SPD conditions. The V_{UFG} for the 2219 Al alloy, however, shows a maximum of about 0.85 at 523 K and decreases with increasing temperature, approaching about 0.5 at 748 K. These values are much larger than those for the Al-3% Cu alloy, as can be seen in Fig. 12. This suggests that dynamic evolution of new grains would be strongly controlled by some material/deformation conditions. The latter will be discussed in the following sections.

4.2.1 Plastic constrain during severe deformation

It is found in the present study that any deformation heterogeneities that result in development of MSBs are

expected to play an important role in grain refinement by severe deformation. It is known that inhomogeneous characteristics may lead to formation of MSBs due to relaxation of strain gradients introduced by ECAP.[4,9,12,16,18] It should be noted that MSBs may be developed in grain interiors due to various kinds of plastic constrains, which may be resulted from deformation/material conditions, for instance, ECAP channel and strain compatibility requirements by neighboring grains, etc. During cold-to-warm deformation, the formation of MSBs occurs because it is easier for a grain to deform if it is split into MSBs, where the number of slip systems required for constrained deformation are fewer than 5.[14,31] The MSBs may also be formed by grain subdivision as a result of microshear banding that is caused by an intrinsic structure instability.[3,30,31] Some external constrains may also appear on macroscopic level, as an inevitable consequence of interaction between sample and tool, *e.g.* due to friction in metalworking process. It is obvious that when a sample is deformed complying with any external constrains, different macroscopic strains should be developed in various parts; this may lead to a strong inhomogeneous deformation in a whole volume as well as grain interiors and thus, to development of the microstructural inhomogeneity followed by formation of MSBs.

4.2.2 Deformation temperature

It is known that the structural heterogeneity introduced by plastic deformation generally decreases with increase in deformation temperature. First, an increase in number of operating slip systems gives rise to more homogeneous deformation. Second, grain boundary sliding (GBS) can result in a high rate of relaxation processes operating in matrices with heterogeneous microstructures. Third, precipitation particles in the aluminum alloys are dissolved in matrix, although dispersion particles can exist stably. This will be discussed in more details in the next section. Fourth, the deformed microstructure becomes rather unstable at high temperatures due to frequent operation of dynamic restoration, such as dynamic recovery and even recrystallization. As the results, the number of grains having large-scale MSBs can be gradually decreased at elevated temperatures[32,33] and then fine-grained microstructures with HABs are hardly developed in the original coarse grains containing subgrains with LABs (see Fig. 9).

4.2.3 Second phase particles

It is seen that coarse second phase precipitates of Al_2Cu phase are distributed in grain interiors in the present Al-3%Cu alloy after overageing treatment (Fig. 1) and numerous MSBs are formed close to the regions containing rich second phase particles[11,12] (Fig. 2). These precipitates are fragmented after ECAP and developed homogeneously in elongated subgrains and along the subboundaries (Fig. 8). These particles may reprecipitate along strain-induced boundaries and can restrict rearrangement of lattice dislocation in short and long range, leading to stabilization of developed dislocation substructures and then rapid formation of MSBs.[12] This may more effectively work at high temperatures ($T > 0.5\ T_m$) despite operation of dynamic recovery, leading to dislocation annihilation within (sub)-grains. It can be concluded, therefore that such high-density fine particles can retard or prevent any relaxation of strain gradients,[9,11,12,24,25] resulting in rapid increase in misorientation of strain-induced boundaries, followed by formation of new grains with HABs.

In contrast to the dilute Al-3%Cu alloy, the 2219 Al alloy contains various alloying elements with moderate concentrations and several secondary phase particles, as well as some dispersion particles (Al_3Cr, Al_6Mn, Al_3Zr).[19,20] Thus, grain refinement process in this alloy may occur more readily because several second phase particles including dispersoids in the 2219 Al alloy can effectively stabilize high-density dislocation microstructures introduced by ECAP and so, deformation-induced microstructures in such alloys can be more stable for a long period of processing time during hot ECAP. This should result in a smaller grain size and a larger average misorientation and a larger volume fraction of fine grains developed at the same deformation temperature (Figs. 11 and 12).

4.2.4 Static restoration during ECAP

An important feature of the ECAP technique at elevated temperatures is that the ECAPed samples inevitably undergo static annealing during repeated ECAP. The developed microstructures should be affected by not only severe deformation, but also static annealing, taking place due to the following reasons.[13,18] First, it is not possible to quench the sample immediately after its transition through the deformation zone. The shear deformation occurs by ECAP only in the intersection plane of channels, while the material remains under static annealing conditions inside heated die at deformation temperature. Second, static annealing also occurs at intervals of time between ECAP passes, since deformation temperature should be maintained or periodically restored during the process. This is inherent to the cyclic deformation mode of ECAP. The present data in Fig. 9(c) imply that such static annealing, resulting in static recovery and, sometimes, static recrystallization, may exercise the significant influence on the deformation microstructure of Al-3%Cu alloy, especially comparing with that of the AA2219 *during* ECAP (see Figs. 11 and 12). Static restoration processes may effectively decrease the strain gradients and/or strain heterogeneities accumulated in each ECAP pass at elevated temperatures[31] and thus, provide incomplete grain refinement even at large strains achieved by ECAP.

5. Conclusions

The microstructure evolution, taking place during ECAP at elevated temperatures, was investigated in a binary Al-3%Cu alloy. The influence of increasing deformation temperature on formation of strain-induced grains was studied in the temperature interval from 523 to 748 K. The main results can be summarized as following.

(1) ECAP of Al-3%Cu alloy results in partial grain refinement at all the pressing temperatures, leading to non-uniform development of deformation-induced fine grains with HABs and the remnant original grains containing subgrains with LABs.

(2) Fine-grained structure is developed by initial grain subdivision due to formation of microshear bands having moderate angle misorientation. The number

and the average misorientation angle of these boundaries increase with deformation, finally leading to development of new fine grains along microshear bands.

(3) The volume fraction and the average misorientation angle of deformation-induced grains are reduced with rising temperature, since inhomogeneous microstructures are hardly developed during hot deformation due to dissolution of precipitates as well as frequent operation of dynamic recovery.

(4) Second phase particles in Al alloys can serve as very effective stabilizers for deformation-induced microstructures, which are developed during and after cyclic ECAP at elevated temperatures.

Acknowledgment

The authors acknowledge with gratitude the financial supports received from the Ministry of Education, Culture, Sports, Science and Technology on Priority Areas "Giant Straining Process for Advanced Materials Containing Ultra-High Density Lattice Defects" and the Light Metals Education Foundation in Japan. One of the authors (I.M.) wishes to thank DAAD for the possibility to perform part of this work in IMM-RWTH Aachen, Germany, and the Japanese government for providing the scholarship. The other one (O.S.) would like to thank the UEC Tokyo for providing a scientific fellowship.

REFERENCES

1) R. Z. Valiev, R. K. Islamgaliev and I. V. Alexandrov: Progr. Mater. Sci. **45** (2000) 103–189.
2) Y. Iwahashi, Z. Horita, M. Nemoto and T. G. Langdon: Acta Mater. **45** (1997) 4733–4741.
3) F. J. Humphreys, P. B. Prangnell, J. R. Bowen, A. Gholinia and C. Harris: Phil. Trans. R. Soc. A **357** (1999) 1663–1681.
4) J. P. Bowen, P. B. Prangnell and F. J. Humphreys: Proc. 20th Risø International Symposium, ed. by J. B. Bilde-Sørensen, J. V. Carstensen, N. Hansen, D. Juul Jensen, T. Leffers, W. Pantleon, O. B. Pedersen and G. Winther, (Risø Lab., Roskilde, Denmark, 1999), p. 269.
5) A. Yamashita, D. Yamaguchi, Z. Horita and T. G. Langdon: Mat. Sci. Eng. A **287** (2000) 100–106.
6) C. Pithan, T. Hashimoto, M. Kawazoe, J. Nagahora and K. Higashi: Mat. Sci. Eng. A **280** (2000) 62–68.
7) J. Y. Chang, J. S. Yoon and G. H. Kim: Scr. Mater. **45** (2001) 347–354.
8) U. Chakkingal and P. F. Thomson: J. Mater. Proc. Tech. **117** (2001) 169–177.
9) A. Goloborodko, O. Sitdikov, T. Sakai, R. Kaibyshev and H. Miura: Mater. Trans. **44** (2003) 766–774.
10) Y. C. Chen, Y. Y. Huang, C. P. Chang and P. W. Kao: Acta Mater. **51** (2003) 2005–2015.
11) P. J. Apps, J. R. Bowen and P. B. Prangnell: Acta Mater. **51** (2003) 2811–2822.
12) A. Goloborodko, O. Sitdikov, R. Kaibyshev, H. Miura and T. Sakai: Mat. Sci. Eng. A **381** (2004) 121–128.
13) M. Popovic and B. Verlinden: Mater. Sci. Technol. **21** (2005) 606–612.
14) P. J. Apps, M. Berta and P. B. Pragnell: Acta Mater. **53** (2005) 499–511.
15) Z. Zhang, S. Hosoda, I.-S. Kim and Y. Watanabe: Mater. Sci. Eng. A **425** (2006) 55–63.
16) O. Sitdikov, T. Sakai, E. Avtokratova, R. Kaibyshev, Y. Kimura and K. Tsuzaki: Mat. Sci. Eng. A **444** (2007) 18–30.
17) J. Gubicza, I. Schiller, N. Q. Chinh, J. Illy, Z. Horita and T. G. Langdon: Mat. Sci. Eng. A **460–461** (2007) 77–85.
18) O. Sitdikov, T. Sakai, E. Avtokratova, R. Kaibyshev, K. Tsuzaki and Y. Watanabe: Acta Mater. **56** (2008) 821–834.
19) I. Mazurina, T. Sakai, H. Miura, O. Sitdikov and R. Kaibyshev: Mat. Sci. Eng. A **473** (2008) 297–305.
20) I. Mazurina, T. Sakai, H. Miura, O. Sitdikov and R. Kaibyshev: Mat. Sci. Eng. A **486** (2008) 662–671.
21) R. Z. Valiev, Y. V. Ivanisenko, E. F. Rauch and B. Baudelet: Acta Mater. **44** (1996) 4705–4712.
22) A. Belyakov, T. Sakai, H. Miura and K. Tsuzaki: Phil. Mag. A **81** (2001) 2629–2643.
23) R. M. Imaev, G. A. Salishchev, O. N. Senkov, V. M. Imayev, M. R. Shagiev, N. K. Gabdullin, A. V. Kuznetsov and F. H. Froes: Mater. Sci. Eng. A **300** (2001) 263–277.
24) O. Sitdikov, T. Sakai, A. Goloborodko and H. Miura: Scripta Mat. **51** (2004) 175–179.
25) O. Sitdikov, T. Sakai, A. Goloborodko, H. Miura and R. Kaibyshev: Phil. Mag. **85** (2005) 1159–1175.
26) S. Ringeval, D. Piot, C. Desrayaud and J. H. Driver: Acta Mater. **54** (2006) 3095–3105.
27) C. Kobayashi, T. Sakai, A. Belyakov and H. Miura: Phil. Mag. Lett. **87** (2007) 751–766.
28) T. Sakai, A. Belyakov and H. Miura: Met. Mat. Trans. **39A** (2008) 2206–2214. doi: 10.1007/s11661-008-9556-8.
29) *Metals Handbook: Metallography, Structures and Phase Diagrams*, ed. by T. Lyman (American Society of Metals, 8, 1973) pp. 163–168.
30) P. J. Hurley and F. J. Humphreys: Acta Mater. **51** (2003) 1087–1102.
31) F. J. Humphreys and M. Hatherly: *Recrystallization and Related Annealing Phenomena, 2nd Edition*, (Elsevier, 2004) pp. 451–467.
32) E. Ball and F. J. Humphreys: *Thermomechanical Processing (TMP^2)*, ed. by W. B. Hutchinson, *et al.*, (ASM, Ohio, 1996) pp. 184.
33) A. Duckham, R. D. Knutsen and O. Engler: Acta Mater. **49** (2001) 2739–2749.